ANALYSIS OF $\pi^-\pi^+$ SCATTERING IN $\pi^+p \to \pi^-\pi^+\pi^+p$ INTERACTIONS[*]

Ernest Malamud,[†] Peter E. Schlein, and T. G. Trippe[‡]
University of California, Los Angeles

and

D. Brown and G. Gidal
Lawrence Radiation Laboratory, Berkeley

August 12, 1969

ABSTRACT

Approximately 19,000 events of the type $\pi^+p \to \pi^-\pi^+\pi^+p$ produced at pion momenta ranging from 3.2 GeV/c to 8.4 GeV/c have been compiled from various groups. The data are dominated by the well-known peripheral ρN^{*++} production. An analysis of the $\pi\pi$ scattering has been performed, yielding values for the T = 0 s-wave phase shift in agreement with those recently obtained in an analysis of $\pi^-p \to \pi^-\pi^+n$. The results reinforce the earlier conclusions that there exists a T = 0 scalar meson $\sigma(730)$.

We present here a $\pi\pi$ phase shift analysis using the reaction

$$\pi^+ p \to \pi^+ \pi^- N^{*++}. \tag{1}$$

The basic sample of 18,593 $\pi^+ p \to \pi^+ \pi^- \pi^+ p$ events was compiled[1] from several laboratories. The distribution of beam momentum and total center-of-mass energy, E^*, for this sample is shown in Fig. 1(a).

The method[2] (referred to hereafter as I) used in the analysis has as its essential feature that prior knowledge of the helicity amplitude magnitudes is not assumed. In a previous application[3] of this method (referred to hereafter as II) to the final state

$$\pi^- p \to \pi^+ \pi^- n, \tag{2}$$

the sample was sufficiently large that the data could be divided into three regions of the $\pi\pi$ center-of-mass production cosine, θ_{CM}, and the spherical harmonic moments, $<Y_L^M>$, evaluated in the $\pi\pi$ rest frame as a function of $\pi\pi$ effective mass, $m_{\pi\pi}$, separately for each of these θ_{CM} regions. Thus the $\pi\pi$ helicity amplitudes in reaction (2) as well as the $\pi\pi$ phase shifts could be extracted from the data using the method outlined in I. The constraints discussed in I were very well satisfied for $600 < m_{\pi\pi} < 900$ MeV, a result which lends much credence to the validity of the analysis.

Although in the analysis presented here we start with a relatively large sample of events, the selection of the N^{*++} (we use $1160 < m_{\pi^+ p} < 1300$ MeV) leaves us with a much reduced sample of reaction (1).

We thus do not attempt here a detailed study as a function of momentum transfer t to the N^*, but simply consider the sample for $t < 0.3\,\mathrm{GeV}^2$. The following points summarize the results obtained in this analysis.

(1) The same three $T = 0$ s-wave $\pi\pi$ phase shift solutions found in II are found for reaction (1). The solution (constant $\delta_s^o \sim 90^\circ$) with the worst confidence level is the one that we concluded in II was unlikely from comparison with $\pi^o\pi^o$ mass spectra.[4] Thus, these results, aside from providing us with good evidence that we are actually measuring $\pi\pi$ phase shifts and not something characteristic of reactions (1) or (2), reinforce the conclusions of II that there exists a $T = 0$ scalar meson $\sigma(730)$.

(2) The ρ parameters obtained in the best fit to reaction (1) agree well with those obtained in II in the fit to reaction (2). This result, in contrast to the results of Roos[5] obtained in fitting mass spectra alone of reaction (1) and (2), is understandable in that the ratio of s- to p-wave $\pi\pi$ systems formed in reaction (1) is not the same as in reaction (2). In fact we would expect this ratio to depend on E^* and t as well as on the reaction type. Thus the varying amount of s/p wave relative contribution to Roos' mass spectra would be sufficient cause for his observed effects.

(3) As a means of obtaining additional confidence in the one-pion-exchange nature of reaction (1), we have examined the $p\pi^+$ scattering angle at the N^{*++} vertex as a function of $m_{p\pi^+}$ in the manner described by Gellert et al.[6] The scattering angle is taken between the initial

state proton and the final state proton as seen in the $\pi^+ p$ rest frame.

Figure 2 shows the $< \mathcal{Y}_\alpha^0 >$ moments of this angular distribution as a

function of $\pi^+ p$ effective mass $m_{\pi^+ p}$ from 1100-2000 MeV. Superim-

posed on these data points are the real particle $\pi^+ p$ elastic scattering

results as summarized in Gellert et al.[6] Agreement is found for $m_{\pi^+ p}$

$\lesssim 1600$ MeV,[7] a situation which lends support to the validity of the one-

pion-exchange description.

As discussed in I, the joint distribution for the scattering at the

$\pi\pi$ and $\pi^+ p$ vertices can be written as

$$D(\hat{q}, \hat{r}) = \sum_{\substack{L,M \\ \mathcal{L},m}} C_{LM}^{\mathcal{L}m} Y_L^M(\hat{q}) \, \mathcal{Y}_\mathcal{L}^m(\hat{r}), \tag{3}$$

in which $\hat{q}$ and $\hat{r}$ are the unit outgoing vectors defined in the $\pi\pi$ and

N^{*++} systems, respectively, of reaction (1). Here we take the coor-

dinate systems in each of these systems to have the $\hat{y}$ axis along the

normal to the production plane $\hat{n} \sim \hat{P}_{in} \times \hat{N}^{*++}$ and the $\hat{z}$ axis in each

case along the helicity axis (i.e. direction of motion) of the $\pi\pi$ or N^*

system, as the case may be. With the N^{*++} selection $1.16 < m_p < 1.30$

GeV in reaction (1), P3/2 dominates and only $\mathcal{L} = 0,2$ need be considered

at this vertex.[8] As in II, we assume only s- and p-wave scattering for

the $\pi\pi$ interaction in the mass range considered $600 < m_{\pi\pi} < 1000$ MeV;

thus we consider here only L = 0, 1, 2.[9]

The $C_{LM}^{\mathcal{L}m}$ coefficients in Eq. (3) given by the experimental quan-

tities in Eq. (4) are shown in I to contain a dependence on the $\pi\pi$

scattering amplitudes determined only by the L value of the moment

(the Y_L^M moment in the $\pi\pi$ system). Thus, all $L = 0$ moments are linear

superpositions of $|A_{\pi\pi}^S|^2$ and $|A_{\pi\pi}^P|^2$, all $L = 1$ moments $\sim \mathrm{Re}\left(A_{\pi\pi}^S A_{\pi\pi}^{P^*}\right)$

and all $L = 2$ moments $\sim |A_{\pi\pi}^P|^2$. The coefficients of these quantities are

the helicity amplitude factors defined in I. To the extent that the helicity

amplitudes are independent of $\pi\pi$ mass over the range considered, the

experimental quantities of Eq. (4) directly reflect the $m_{\pi\pi}$ dependence of

the $\pi\pi$ scattering amplitudes. We find that the tests suggested in I are

well satisfied by the complete set of moments, namely that all moments

of the same L are compatible with having the same $m_{\pi\pi}$ dependence.

Some of these moments are shown in Fig. 3.

Despite the large amount of information contained in the complete

set of correlation moments, the major contribution still comes from

the $N\langle Y_1^0 \mathcal{Y}_0^0 \rangle$ and $N\langle Y_2^0 \mathcal{Y}_0^0 \rangle$ moments. We report here the results

of an analysis in which we fit the data to the equations[10]

$$N = K_1 |A_{\pi\pi}^S|^2 + K_2 |A_{\pi\pi}^P|^2 \tag{4a}$$

$$N\langle Y_0^0 \mathcal{Y}_2^0 \rangle = K_3 |A_{\pi\pi}^S|^2 + K_4 |A_{\pi\pi}^P|^2 \tag{4b}$$

$$N\langle Y_0^0 \mathrm{Re}\, \mathcal{Y}_2^1 \rangle = K_5 |A_{\pi\pi}^S|^2 + K_6 |A_{\pi\pi}^P|^2 \tag{4c}$$

$$N\langle Y_0^0 \mathrm{Re}\, \mathcal{Y}_2^2 \rangle = K_7 |A_{\pi\pi}^S|^2 + K_8 |A_{\pi\pi}^P|^2 \tag{4d}$$

$$N\langle Y_1^o \mathcal{Y}_o^o \rangle = K_9 \ \mathrm{Re} \left(A_{\pi\pi}^S A_{\pi\pi}^{P*} \right) \tag{4e}$$

$$N\langle Y_2^o \mathcal{Y}_o^o \rangle = K_{10} \left| A_{\pi\pi}^P \right|^2 . \tag{4f}$$

The data is divided into twenty 20 MeV bins between $600 \le M_{\pi\pi} \le 1000$ MeV yielding 120 independent data points. In addition, we use the twenty $N\langle Y_1^o \rangle$ moments from the reaction $\pi^- p \to \pi^- \pi^o p$ used in the $\pi^- \pi^+ n$ analysis[2] to obtain independent information on the $T = 2$ s-wave interaction. The $\pi^+ \pi^-$ elastic scattering amplitudes are assumed to have the form

$$A_{\pi^- \pi^+}^S = \frac{2}{3} e^{i\delta_s^o} \sin \delta_s^o + \frac{1}{3} e^{i\delta_s^2} \sin \delta_s^2 \tag{5a}$$

$$A_{\pi^- \pi^+}^P = e^{i\delta_p} \sin \delta_p . \tag{5b}$$

The unknowns are therefore: K_1 through K_{10}, δ_s^o in each of the twenty $m_{\pi\pi}$ intervals, δ_s^2 at seven different $m_{\pi\pi}$ values, and two Breit-Wigner parameters, M_ρ and Γ_ρ, for determining the p-wave amplitude using the form:

$$\cot \delta_p = \left[m_\rho^2 - m_{\pi\pi}^2 \right] \left[1 + \left(q/q_\rho \right)^2 \right] / \left[2m_\rho \Gamma_\rho \left(q/q_\rho \right)^3 \right] ,$$

where q_ρ and q are the $\pi\pi$ c.m. decay momenta for $\pi\pi$ systems of mass m_ρ and $m_{\pi\pi}$, respectively. Two additional parameters are

included in order to give a quadratic $m_{\pi\pi}$ dependence to the K_i's as

in II. Finally, the unknown constant multiplying $\text{Re} \left(A_{\pi\pi}^S A_{\pi\pi}^{P*} \right)$ in the

$\pi^- \pi^0 p$ data brings the number of variables in the fit to 42 and the

number of constraints to 98.

The same three solutions found in II are again found in our fits

to reaction (1). These solutions are summarized in Fig. 4 and Table I.

The excellent agreement between the results on reactions (1) and (2)

implies quite strongly that we are indeed measuring properties of the

$\pi\pi$ system rather than of the reactions as a whole. It seems unlikely

that if final-state-interactions or the like were playing a significant

role in reactions (1) and (2) we would find these same solutions.

It was pointed out in II that the more slowly δ_s^0 varies with $m_{\pi\pi}$,

the more important it is not to make false assumptions concerning the

$m_{\pi\pi}$ dependence of the helicity amplitude quantities. The steepness of

the lower Chew-Low boundary [see Fig. 1(b)] for the low E^* events in

the sample could cause difficulties in the fits due to the fact that the t

selection then depends strongly on $m_{\pi\pi}$. Since the helicity amplitudes

do not have the same t dependence in general, this can result in dif-

ferent $m_{\pi\pi}$ dependencies for the K_i's in Eqs. (4), a situation which is

not allowed for in the analysis. Therefore we have rerun the fits using

only the 1179 events for $E^* > 3.5$ GeV, for which this question is less

important as seen in Fig. 1(b). The s- and p-wave phase shift results

are found to be compatible with those for the entire sample; however

the χ^2 for the UP-DOWN solution decreases somewhat. Table I includes

some of the results from these fits. It is seen that the UP-DOWN

solution has a confidence level of 0.1%, a factor of ~ 25 below those

for the UP-UP and DOWN-UP solutions, thereby reinforcing the earlier

unlikelihood of the UP-DOWN solution which was based on the entirely

independent argument of the comparison with the few published exper-

imental mass spectra[4] of the $\pi^o \pi^o$ system all of which show a drop-off

above ~ 800 MeV.

The ρ parameters, m_ρ and Γ_ρ for the preferred UP-UP solution

are 765 ± 4 and 154 ± 8 MeV. These agree well with the values for this

solution found in II in the analysis of reaction (2): 767 ± 2 and 149 ± 5 MeV.

The amount of p-wave to s-wave present in the $\pi\pi$ system before scat-

tering is given in Table I by the column labeled K_2/K_1. Thus it is seen

that for the UP-UP solution, reaction (1) contains more s-wave component

in the mass spectrum than reaction (2), where the comparable ratio was

found to be 3.0 ± 0.2. This may be understood in view of the expectation

that the virtual pion cloud in reaction (1) is smaller than that in reaction

(2), thereby leading to a smaller average effective $\pi\pi$ impact parameter.

FOOTNOTES AND REFERENCES

*Supported in part by the U. S. Atomic Energy Commission.

†Present address: National Accelerator Laboratory, Batavia, Illinois.

‡Present address: CERN, Geneva, Switzerland.

[1] This analysis uses data from the following laboratories and collaborations: Columbia-Rutgers [M. Rabin, R. Plano, C. Baltay, P. Franzini, L. Kirsch, H. Kung, and N. Yeh, Bull. Am. Phys. Soc. $\underline{12}$, 9 (1967).]

Lawrence Radiation Laboratory [D. Brown et al., UCRL-17665 (1967).]

Lawrence Radiation Laboratory [G. Goldhaber et al., Phys. Rev. Letters $\underline{12}$, 336 (1964).]

Rochester-Yale [P. Slattery, H. Kraybill, B. Forman, and T. Ferbel, University of Rochester Report UR-875-153 (1966).]

University of California, San Diego [Maris Abolins et al., Phys. Rev. Letters $\underline{11}$, 381 (1963).]

[2] Peter E. Schlein, Phys. Rev. Letters $\underline{19}$, 1052 (1967).

[3] Ernest Malamud and Peter E. Schlein, Phys. Rev. Letters $\underline{19}$, 1056 (1967).

[4] I. F. Corbett, C. J. S. Damerell, N. Middlemas, D. Newton, A. B. Clegg, W. S. C. Williams, and A. S. Carroll, Phys. Rev. $\underline{156}$, 1451 (1967); Z. S. Strugalski, I. V. Chuvilo, I. A. Ivanovska, L. S. Okhrimenko, B. Niczyporuk, I. Kanarek, B. Stowinski, and Z. Jablonski,

quoted by G. Goldhaber in Proceedings of the XIIIth International

Conference on High Energy Physics, University of California Press,

(1967), p. 108; M. Wahlig, E. Shibata, D. Gordon, D. Frisch, and

I. Mannelli, Phys. Rev. 147, 941 (1966).

[5] M. Roos, CERN Preprint Ref. TH.798, June 26, 1967.

[6] Eugene Gellert et al., Phys. Rev. Letters 17, 884 (1966).

[7] Above about 1600 MeV in π^+p mass the measured moments are too

high. This excessive forward peaking in the π^+p system is presuma-

bly due to the influence of the strong s-wave $\rho\pi$ interaction known as

the A_1.

[8] With this π^+p mass selection, and restricting the momentum transfer

$t \leq 0.3 (GeV/c)^2$ 3.2% of the "events" are actually both combinations

of the same event which satisfy these selection criteria.

[9] As in II, we find no significant evidence for higher order moments in

this $m_{\pi\pi}$ range.

[10] In view of the increased number of helicity amplitude quantities in

reaction (1) due to the spin three halves nature of the N^* we have not

yet attempted to extract the helicity amplitudes as was done in the

$\pi^-\pi^+$n analysis.[2] As discussed in I simultaneous extraction of the

helicity amplitudes and $\pi\pi$ phase shifts would require that the analysis

be performed on data which has been selected in relatively narrow bins

of momentum transfer and possibly center-of-mass energy. Despite

the 19,000 events available in the present analysis, the statistics are

not sufficient for an analysis with that complexity. We therefore per-

form an analysis of the t and E^{*} averaged type discussed in I.

Table I. Phase Shift Solutions.

Solution	Data Used	M Dependence[a] of $K_1 - K_{10}$	K_2/K_1	χ^2 (Constraints = 98)	C. L.	Mρ (MeV)	$\Gamma\rho$ (MeV)
DOWN-UP	All	$1-0.01\Delta-0.96\Delta^2$	1.1 ± 0.8	125	0.041	766 ± 9	167 ± 13
UP-UP	All	$1+0.03\Delta-0.98\Delta^2$	1.9 ± 0.5	123	0.046	765 ± 4	154 ± 8
UP-DOWN	All	$1-0.85\Delta-1.40\Delta^2$	5.1 ± 1.3	167	$<10^{-4}$	762 ± 4	158 ± 4
DOWN-UP	E. C. M.	$1+0.00\Delta-0.99\Delta^2$	1.2 ± 0.6	128	0.023	766 ± 8	160 ± 14
UP-UP	< 3.5	$1+0.01\Delta-1.01\Delta^2$	4.0 ± 1.3	127	0.025	765 ± 4	149 ± 8
UP-DOWN	GeV	$1-0.9\Delta-1.0\Delta^2$	5.7 ± 1.9	147	0.001	758 ± 3	140 ± 2

[a] $\Delta = M_{\pi\pi} - 0.750$ GeV

FIGURE CAPTIONS

Fig. 1. (a) Distribution of total center-of-mass energy for the combined sample of events. (b) The lower boundary of the Chew-Low plot for various E^* in the sample shows how the $M_{\pi\pi}$ dependence of the helicity amplitudes can be expected to differ for events having different E^*. (c)(d) Momentum transfer distribution for the 4193 events used in the analysis. The two E^* regions are plotted separately.

Fig. 2. $\langle \mathcal{Y}_\ell^m \rangle$ moments of the π^+p scattering distribution as a function of π^+p effective mass. The curves are derived from the real particle π^+p elastic scattering experiments.

Fig. 3. (a) The $\pi\pi$ mass histogram and the "correlated mass spectra," (i.e. the $\mathcal{L}$ = 2 moments at the π^+p vertex multiplied by the mass histogram) shown as a function of $\pi\pi$ mass. These four sets of data were used in the fits. (b) The uncorrelated moments at the $\pi^-\pi^+$ vertex multiplied by the mass histogram. Only the M = 0 sets of points were used in the fits.

Fig. 4. δ_s^o and δ_s^2 as a function of $\pi\pi$ mass for the three solutions discussed in the text.
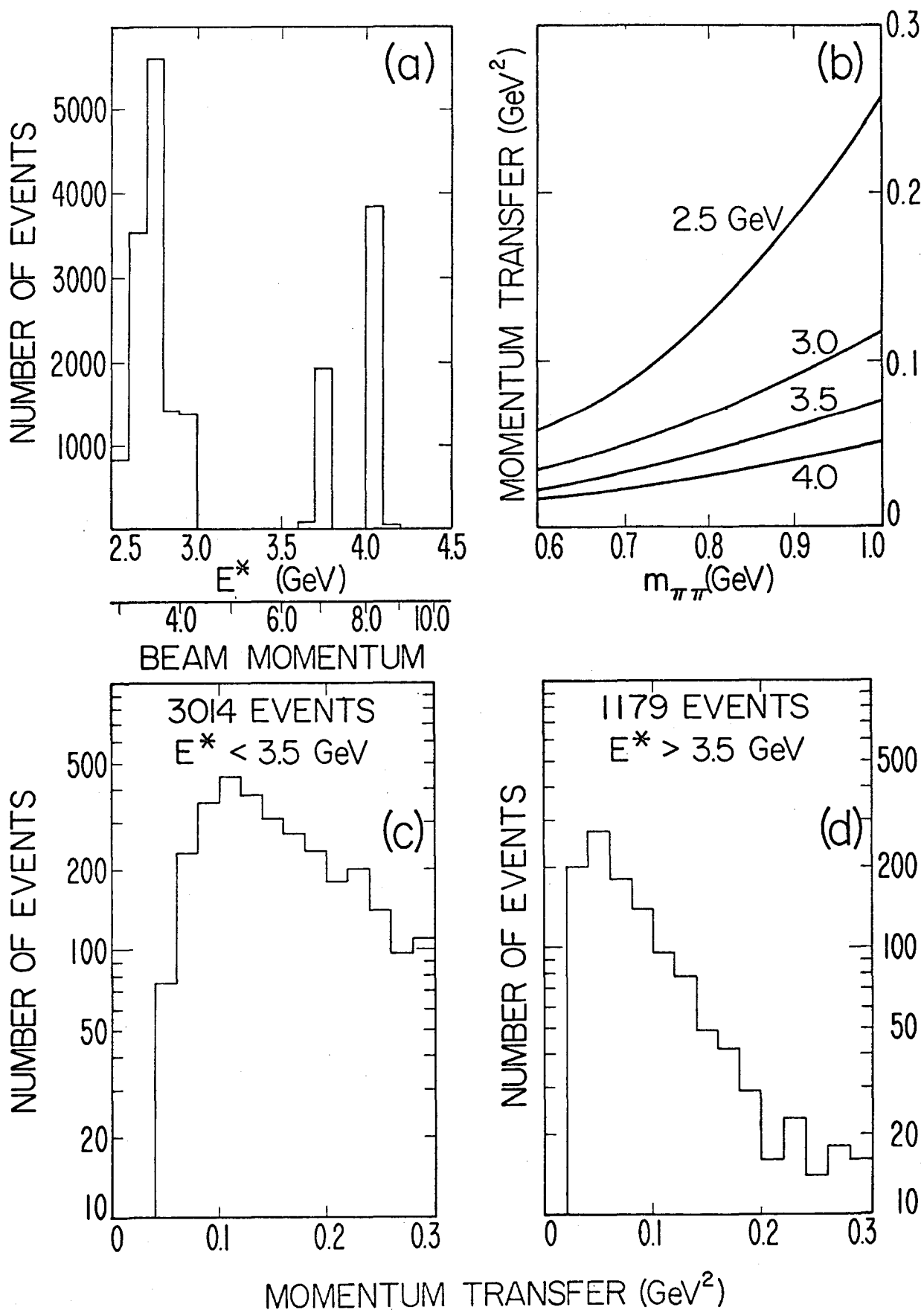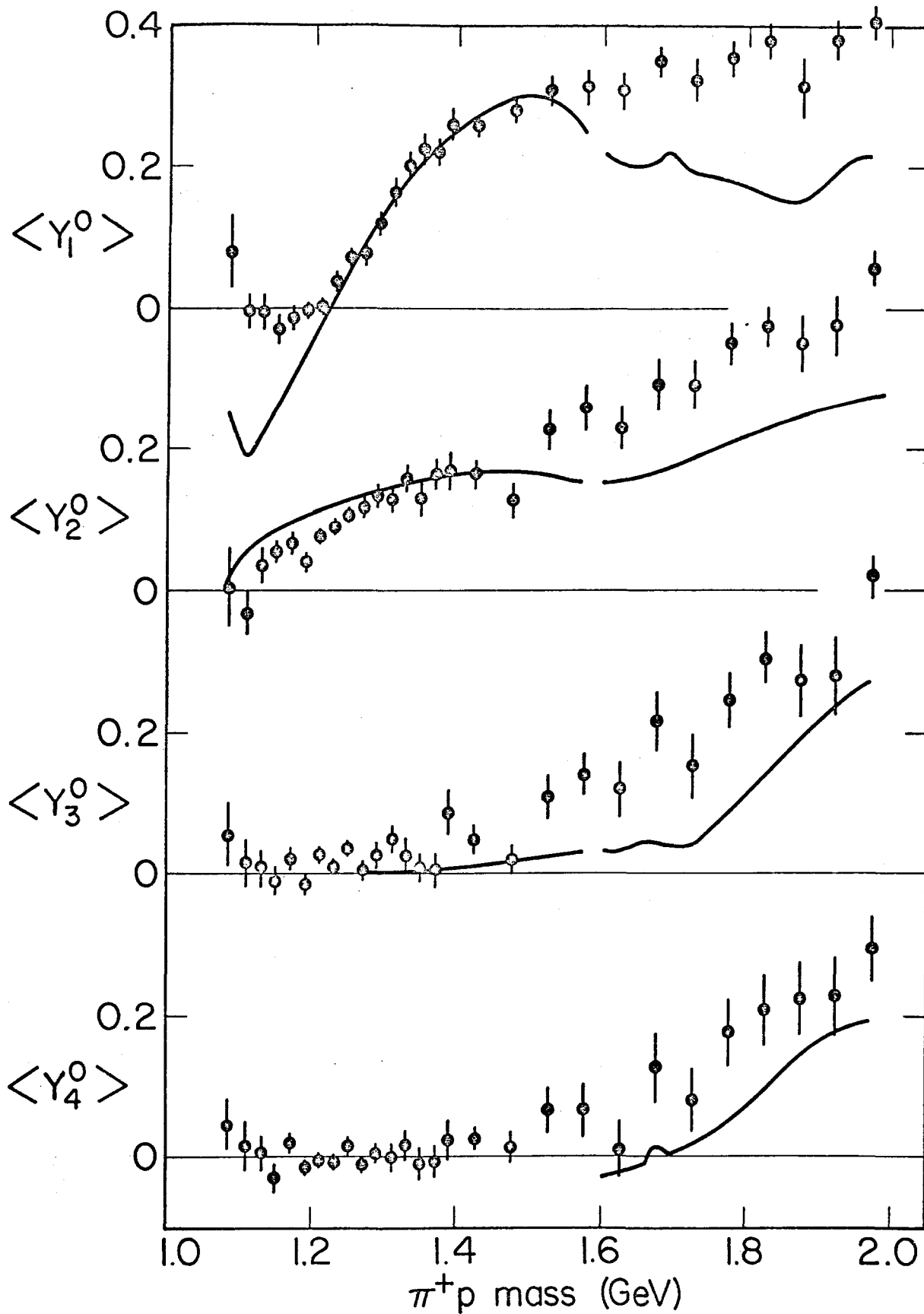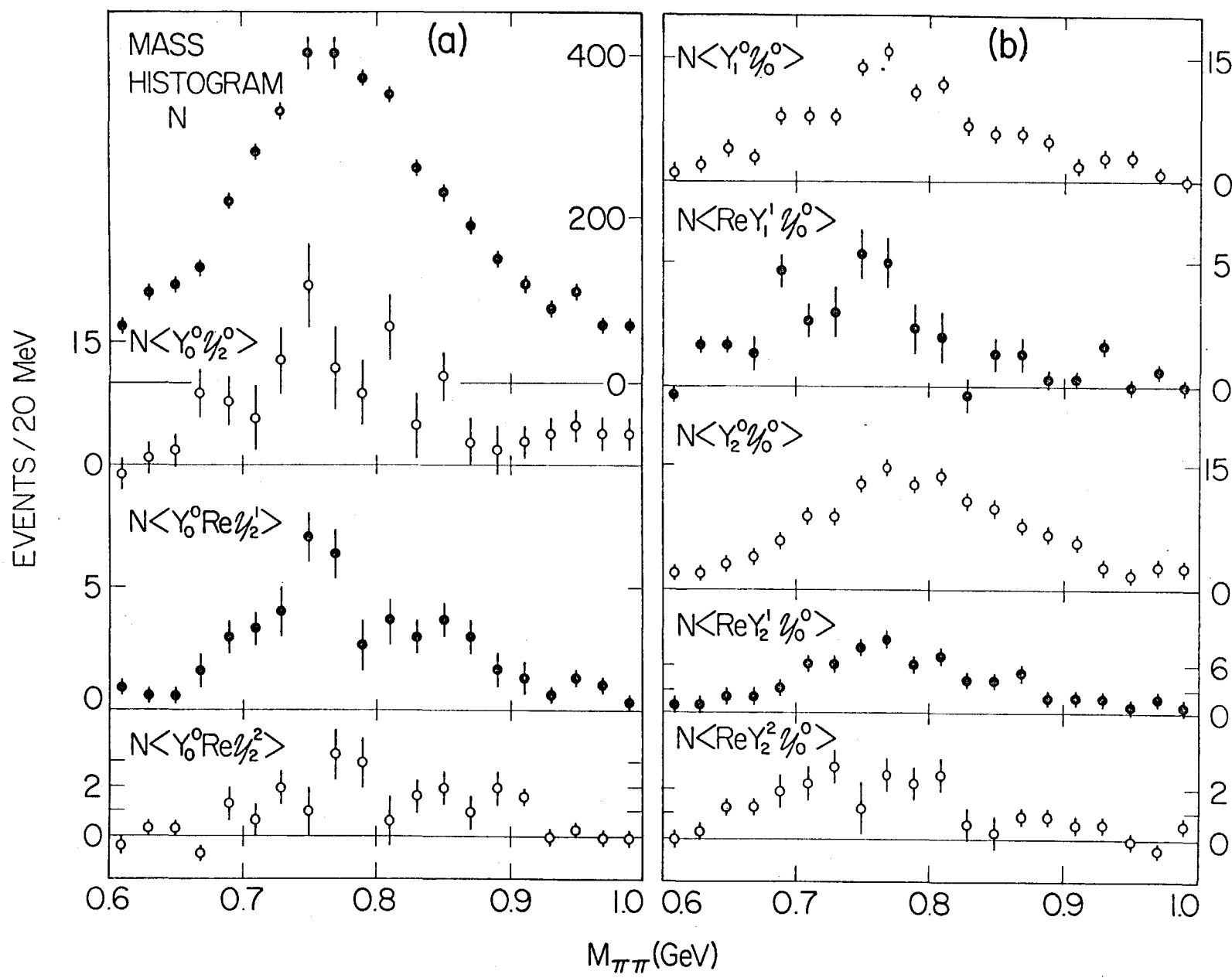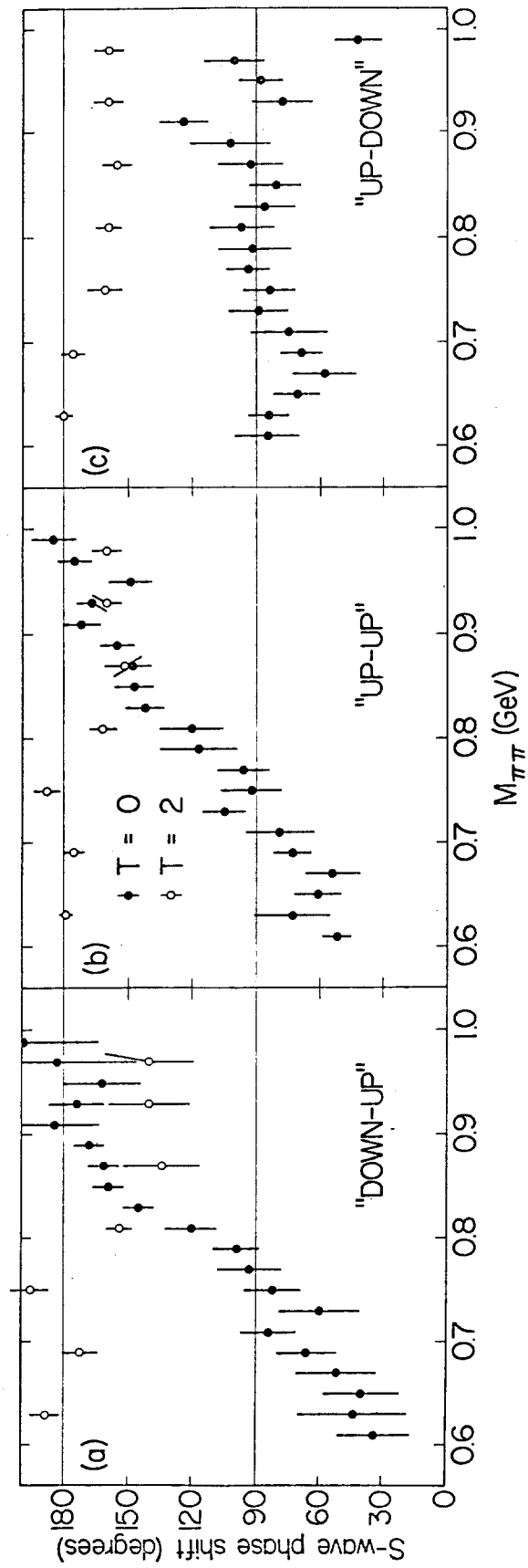
Fig. 1

Fig. 2

EVENTS/20 MeV

MASS HISTOGRAM N (a)

$N\langle Y_1^0 \mathcal{Y}_0^0 \rangle$ (b)

$N\langle Y_0^0 \mathcal{Y}_2^0 \rangle$

$N\langle ReY_1^1 \mathcal{Y}_0^0 \rangle$

$N\langle Y_0^0 Re\mathcal{Y}_2^1 \rangle$

$N\langle Y_2^0 \mathcal{Y}_0^0 \rangle$

$N\langle Y_0^0 Re\mathcal{Y}_2^2 \rangle$

$N\langle ReY_2^1 \mathcal{Y}_0^0 \rangle$

$N\langle ReY_2^2 \mathcal{Y}_0^0 \rangle$

$M_{\pi\pi}$(GeV)

Fig. 3

Fig. 4